ChemComm

COMMUNICATION

View Article Online
View Journal | View Issue

Cite this: *Chem. Commun.*, 2020, **56**, 5366

Received 11th February 2020,
Accepted 6th April 2020

DOI: 10.1039/d0cc01092h

rsc.li/chemcomm

Organic "receptor" fully covered few-layer organic–metal chalcogenides for high-performance chemiresistive gas sensing at room temperature†

Huijie Jiang,[ab] Linan Cao,[ab] Yanzhou Li,[a] Wenhua Li,[a] Xiaoliang Ye,[a] Weihua Deng,[ab] Xiaoming Jiang,[a] Guane Wang[a] and Gang Xu *[ab]

Organic–metal chalcogenides (OMCs) are proposed as a new family of two-dimensional (2D) chemiresistive sensing materials. Few-layer Ag(SPh-NH_2), one of the OMCs, fully and orderly covered with predesigned $-NH_2$ groups as "receptors", shows the highest sensitivity, excellent selectivity and reversibility in response to NO_2 among all the reported 2D chemiresistive sensing materials at room temperature.

Chemiresistors have attracted intensive research interest due to their fascinating features, such as high sensitivity, fast response, low fabrication cost, and real-time detection. Metal oxides are the dominant and key sensing materials for chemiresistive sensors. However, the applications of metal oxide sensors are significantly hampered by their unsatisfying selectivity and high operating temperature.[1–3] Therefore, it is of great importance to develop new sensing materials that possess high sensitivity and selectivity toward target gases for room temperature (RT) operation.

Two-dimensional (2D) materials, such as graphene and its derivatives,[4,5] transition metal dichalcogenides (TMDs),[6–8] black phosphorus (BP),[7–10] 2D metal–organic frameworks (MOFs),[11–20] 2D covalent-organic frameworks (COFs),[21] *etc.*, have obtained increasing attention as chemiresistive gas sensing materials.[22] Compared with their bulk counterparts, 2D materials possess fascinating features for gas sensing, such as a larger surface-to-volume ratio, more accessible active sites, better charge transport, and good processability,[23] which endow the thin films made from them with good gas sensing performance at RT.[19,20,24,25] We noticed that the sensitivity and selectivity of these 2D materials were significantly enhanced by modifying their surfaces with organic functional groups due to the enhanced interactions between 2D materials and target gases.[26–28] For example, Shi's group reported that sulfanilic acid and ethylenediamine (S–G, EDA–G) treated reduced graphene oxide (rGO) materials showed 16.4 and 4.3 times higher responses to NO_2 than that of pristine rGO, respectively.[26] Compared with non-functionalized rGO, chemically fluorinated GO (CFGO) displayed enhanced selectivity between NH_3 and NO_2 by 3.65 times.[28] However, the known post-treated 2D materials normally have a relatively low amount of modified surface and inhomogeneous distribution of functional groups. This profoundly hinders us from achieving higher sensing performances with the known 2D materials and their derivatives.

Recently, a new type of semiconducting 2D materials, organic–metal chalcogenides (OMCs), has emerged.[29,30] Compared to other 2D materials, the surfaces of OMCs are fully and orderly covered by organic functional groups. Our previous work revealed that the conductivity of OMCs is very sensitive to the electronic structure of these organic groups. A change of 10^6 times in their conductivity was observed when varying the type of organic groups on them. Since the electronic structure of these organic groups would be influenced after adsorbing foreign gas molecules, we proposed that OMCs may possess high sensitivity as a chemiresistive sensing material at RT. More importantly, these organic functional groups of OMCs can be designed with the required structure to enhance their affinity to the target gas. Therefore, a "made to order" selectivity that is desired for sensing materials may be realized in OMCs.

Herein, we report the first study of OMCs that possess a very high amount of organic functionalized surface as highly sensitive and selective RT chemiresistive gas sensing materials. As a proof-of-concept, a few-layer OMC, Ag(SPh-NH_2), was prepared for detecting NO_2. The 2D $\{AgS\}_n$ layers of Ag(SPh-NH_2) are fully covered by ordered $-NH_2$ groups. This design remarkably enhanced the sensitivity and selectivity of OMCs to NO_2 as $-NH_2$ groups can be regarded as "receptors" that strongly

[a] *State Key Laboratory of Structural Chemistry, Fujian Institute of Research on the Structure of Matter, Chinese Academy of Sciences (CAS), No. 155 Yangqiao Road West, Fuzhou, Fujian, 350002, P. R. China. E-mail: gxu@fjirsm.ac.cn*
[b] *University of Chinese Academy of Sciences (UCAS), No. 19A Yuquan Road, Beijing 100049, P. R. China*

† Electronic supplementary information (ESI) available: Experimental details, Fig. S1–S18 and Tables S1–S4. See DOI: 10.1039/d0cc01092h

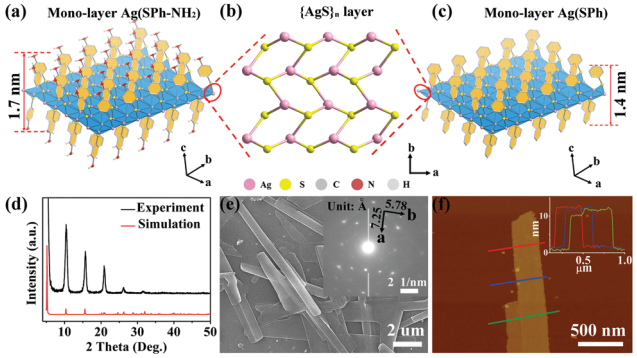

Fig. 1 (a and c) Mono-layer structures of Ag(SPh-NH_2) and Ag(SPh). (b) 2D $\{AgS\}_n$ layer of Ag(SPh-NH_2) and Ag(SPh). Hydrogen atoms of the benzene ring have been omitted for clarity. (d) Experimental and simulated PXRD patterns of Ag(SPh-NH_2). (e) SEM image of few-layer Ag(SPh-NH_2), inset is its selected area electron diffraction pattern. (f) Typical AFM image of few-layer Ag(SPh-NH_2).

interact with NO_2 through hydrogen bonding, acid–base interaction, *etc*. As a result, at RT, the few-layer Ag(SPh-NH_2) thin film showed not only the highest sensitivity and fastest response and recovery speed among all the reported 2D chemiresistive sensing materials and their modified derivatives, but also very unique selectivity among 12 commonly existing interference gases.

Few-layer Ag(SPh-NH_2) was directly synthesized by the coordination reaction between Ag ions and HSPh-NH_2 (4-aminobenzenethiol) under hydrothermal conditions at 85 °C. For control experiments, Ag(SPh) (HSPh = benzenethiol), an isostructure of Ag(SPh-NH_2), was prepared with a similar synthetic method (for experimental details, see ESI†). The experimental powder X-ray diffraction (PXRD) patterns of Ag(SPh-NH_2) and Ag(SPh) are in good agreement with their simulated or reported ones, verifying their phase purity (Fig. 1d and Fig. S1, ESI†).[31] Fourier transform infrared spectroscopy (FT-IR) and elemental analysis measurements further confirmed their structures and purities (Fig. S2, S3 and Table S1, ESI†).

In the structure of mono-layer Ag(SPh-NH_2) and Ag(SPh) (Fig. 1a and c), each Ag^+ ion coordinates with three μ_3-bridging S atoms in a trigonal planar configuration to form a distorted honeycomb 2D $\{AgS\}_n$ layer (Fig. 1b). The organic functional groups alternatively and covalently bond to S atoms on the top and bottom surfaces of the $\{AgS\}_n$ layer. The thickness of mono-layer Ag(SPh-NH_2) and Ag(SPh) is ~1.7 nm and 1.4 nm, respectively. These mono-layers parallelly pack with each other along the *c* axis to form few-layer Ag(SPh-NH_2) and Ag(SPh) (Fig. S4 and S5, ESI†). The +1 valence of Ag was confirmed by high-resolution X-ray photoelectron spectroscopy (XPS) spectra of few-layer Ag(SPh-NH_2) and Ag(SPh). Meanwhile, the binding energy of N1s for Ag(SPh-NH_2) was determined to be ~400 eV, which is the same as that of phenylamine, suggesting that the amine groups on the surface of few-layer Ag(SPh-NH_2) are accessible to target gas molecules (Fig. S6 and S7, ESI†).[32]

Scanning electron microscopy (SEM) measurements revealed the nanobelt morphology of the as-prepared few-layer Ag(SPh-NH_2) with a length of several micrometers and a width of ~500 nanometers (Fig. 1e). The selected area electron diffraction pattern of TEM showed sharp and ordered spot arrays, indicating the good crystallinity of few-layer Ag(SPh-NH_2) (inset of Fig. 1e). The plane distances were measured to be 7.25 Å and 5.78 Å along the *a* and *b* directions, respectively, which correlate well with the simulated results.[33] Atomic force microscopy (AFM) measurement showed that the average thickness of few-layer Ag(SPh-NH_2) is ~11 nm, indicating the stacking of ~6 molecule layers (Fig. 1f). Likewise, the plate morphology of the as-prepared few-layer Ag(SPh) was confirmed with an average thickness of ~20 nm (Fig. S8 and S9, ESI†).

The electrical and optical characterization results reveal that Ag(SPh-NH_2) is a p-type semiconductor with a conductivity of 6×10^{-7} S cm^{-1} at RT and a band gap of 2.62 eV, respectively.[30] The sensing performance of few-layer Ag(SPh-NH_2) was evaluated by preparing it into thin films on quartz substrates using a conventional spin-coating method and then depositing patterned gold on then as interdigital electrodes *via* thermal evaporation (Fig. 2a, details see ESI†). These thin films have a continuous and homogeneous morphology (Fig. 2b). They also showed similar conductivity and ohmic contact with gold electrodes, indicating their good reproducibility (Fig. 2c). The sensing tests of few-layer Ag(SPh-NH_2) thin films were conducted by putting them into a sealed quartz chamber of a home-made test instrument and recording the current of the sensing material in different atmospheres (for details, please refer to the ESI†).[34] All tests were performed at RT.

NO_2 is one of the major global gas pollutants and very toxic even at low concentrations. The performances of NO_2 sensing materials were reported to be significantly enhanced by decorating the surface of them with $-NH_2$ containing molecules.[26,35] Inspired by this, the few-layer Ag(SPh-NH_2) thin film is expected to show high RT sensing performances, because its surfaces are fully and orderly covered by $-NH_2$ groups, which are effective "receptors" for NO_2. As shown in Fig. 3a, when exposed to 10 ppm NO_2, the current of the few-layer Ag(SPh-NH_2) thin film dramatically increased and reached saturation. After refilling the chamber with dry air, few-layer Ag(SPh-NH_2) recovered to its initial resistance.

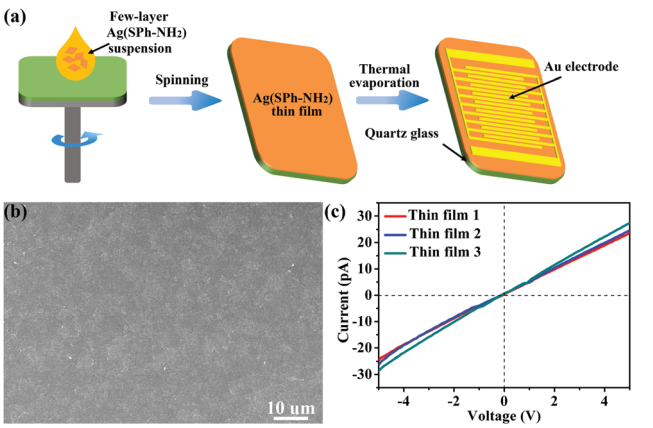

Fig. 2 (a) Fabrication of Ag(SPh-NH_2) thin film for gas sensing test. (b) Typical HR-SEM of the prepared Ag(SPh-NH_2) thin films. (c) *I*–*V* curves of Ag(SPh-NH_2) thin films.

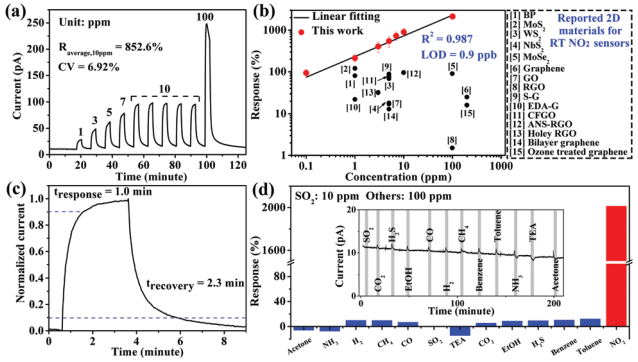

Fig. 3 (a) Response–recovery curve of the Ag(SPh-NH_2) thin film to NO_2 with different concentrations at RT. (b) Linear log–log plot of response *vs.* concentration of the Ag(SPh-NH_2) thin film to NO_2 and a comparison with reported 2D chemiresistive sensing materials working at RT (for details, see Table S3, ESI†). (c) Response-recovery curve to 10 ppm NO_2. (d) Cross-sensitivities of the Ag(SPh-NH_2) thin film to 13 types of gases, inset is the real-time measurement (for details, see Table S4, ESI†).

The response coefficient of variation (CV) is only 6.92% over five continuous cycles, which indicates excellent repeatability (for response values, see Table S2, ESI†). Few-layer Ag(SPh-NH_2) also showed good response–recovery ability in a broad concentration range of NO_2 (0.1–100 ppm) (Fig. 3a and Fig. S13, ESI†). In addition, the Ag(SPh-NH_2) thin film before and after NO_2 sensing tests showed almost the same PXRD patterns (Fig. S14, ESI†), indicating that it is stable in the NO_2 atmosphere. Notably, compared with the reported 2D chemiresistive sensing materials, few-layer Ag(SPh-NH_2) exhibits the highest response to NO_2 throughout the above-mentioned concentration range (Fig. 3b and Table S3, ESI†).

The response-concentration log–log plot of few-layer Ag(SPh-NH_2) is shown in Fig. 3b. The good linearity (R^2 = 0.987) in the range of 0.1–100 ppm is consistent with those of typical chemiresistive sensing materials.[34] Accordingly, the theoretical limit of detection (LOD) was calculated to be 0.9 ppb by setting R = 10%, which is the lowest value among all the reported 2D chemiresistive sensing materials and is good enough to achieve the detection of trace NO_2.[36] Few-layer Ag(SPh-NH_2) also showed a fast response and recovery speed (Fig. 3c). The response and recovery times were calculated to be 1.0 and 2.3 minutes, respectively. These values suggest that few-layer Ag(SPh-NH_2) is the fastest 2D chemiresistive sensing material to NO_2 at RT reported so far (Table S3, ESI†).

The organic ''receptor'' fully covering the structure of few-layer Ag(SPh-NH_2) not only enhanced the sensitivity but also provided excellent selectivity to NO_2 (Fig. 3d). It showed very weak responses (<20%) toward 12 commonly existing interference gases including SO_2, a typical interference gas for NO_2 detection (for response values, see Table S4, ESI†), indicating that few-layer Ag(SPh-NH_2) is capable of selectively distinguishing NO_2 from its interference gases. To shed more light on the relationships between crystal structure and sensing performance, Ag(SPh), a p-type semiconducting isostructure of Ag(SPh-NH_2), was investigated (Fig. 1c and Fig. S15–S17, ESI†). However, different from Ag(SPh-NH_2), Ag(SPh) did not display any observable response to 10 ppm NO_2 (Fig. 4a). This result suggests that $-NH_2$ groups are crucial for detecting NO_2. To uncover more details, *in situ* diffuse reflectance infrared Fourier transform spectroscopy (DRIFTS) measurements were performed by exposing Ag(SPh-NH_2) to a NO_2 atmosphere to study the interactions (Fig. 4b and Fig. S18, ESI†). With increasing exposure time, the intensity of the peaks for $-NH_2$ vibrations (3380 and 3301 cm^{-1}) and C–N (1251 cm^{-1}) stretching vibration decreased dramatically.[37] The peak at 3190 cm^{-1} decreased obviously, which can be assigned to the overtone of N–H bending vibration. Meanwhile, four new peaks belonging to NO_2 (1505 and 1318 cm^{-1}) and N_2O_4 (1496, 1319 cm^{-1} and 1287, 1224 cm^{-1}, the dimer of NO_2) were observed with increasing intensities upon extending the exposure time.[38,39]

Compared with their gaseous state, the adsorbed NO_2 and N_2O_4 showed a slight shift. Meanwhile, O–H bending vibration at 1591 cm^{-1} was also observed (Fig. 4b).[40] These observations revealed the formation of a hydrogen bond through O atoms of N_2O_4/NO_2 and H atoms of $-NH_2$ groups. During the above process, none of the peaks related to diazonium salt (2280 cm^{-1}) or nitrates (1350 cm^{-1}) was detected,[37,38] indicating a strong adsorption of NO_2 on Ag(SPh-NH_2). Notably, the intensity change of $-NH_2$ and N_2O_4 related peaks was synchronous, which revealed a strong interaction between $-NH_2$ and adsorbed N_2O_4. The above results demonstrated the critical role played by $-NH_2$ groups as a functional motif in the Ag(SPh-NH_2) sensing material.[41,42]

A possible mechanism of NO_2 detection with Ag(SPh-NH_2) is proposed as follows (Fig. 4c): when NO_2 approaches the surface of Ag(SPh-NH_2), it firstly contacts with the $-NH_2$ groups through strong interactions (*e.g.*, acid–base interaction, hydrogen bond)[43] in the form of NO_2/N_2O_4; simultaneously, charge

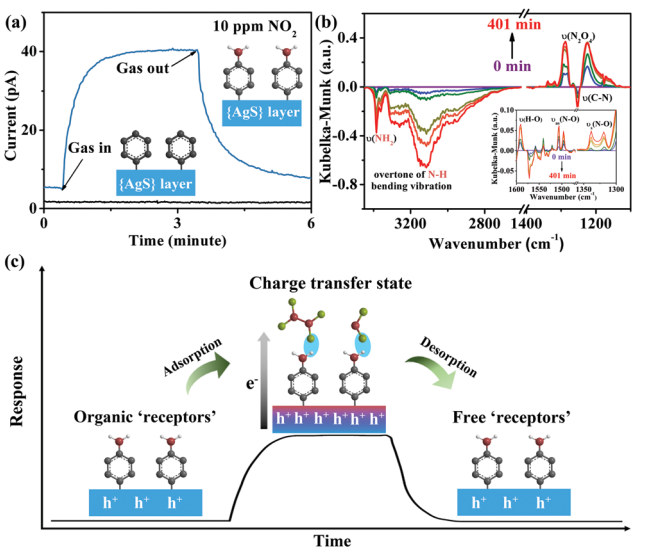

Fig. 4 (a) Response-recovery curves of Ag(SPh-NH_2) (blue) and Ag(SPh) (black) to 10 ppm NO_2. (b) *In situ* DRIFT Spectra for Ag(SPh-NH_2) exposed to NO_2 as a function of time. (c) Possible NO_2 sensing mechanism for Ag(SPh-NH_2).

transfer from Ag(SPh-NH_2) to NO_2 and N_2O_4 would happen, which increases the concentration of hole carriers for p-type Ag(SPh-NH_2); finally, Ag(SPh-NH_2) shows a positive response by increasing its current; once NO_2 and N_2O_4 molecules are swept away by purging gases from the surface of Ag(SPh-NH_2), the current recovers to its initial value.

In conclusion, OMCs, a family of newly emerging inorganic 2D materials, were demonstrated as a kind of designable high-performance RT chemiresitive gas sensing material for the first time. This was realized by preparing few-layer Ag(SPh-NH_2), a member of the OMCs, and applying it for NO_2 detection. Ag(SPh-NH_2) possesses a semi-conducting $\{AgS\}_n$ layer and -NH_2 groups fully and orderly covered on its surface. The comparison of the sensing performances between Ag(SPh-NH_2) and its isostructure, Ag(SPh), and *in situ* DRIFTS measurements of Ag(SPh-NH_2) in a NO_2 atmosphere revealed that the –NH_2 groups are effective ''receptors'' to interact with NO_2 and play the critical role in dramatically enhancing its sensing sensitivity and selectivity. As a result, it shows the highest response value, lowest LOD, and fastest response and recovery speed to NO_2 among all the reported 2D chemiresistive sensing materials at RT. Moreover, it also shows excellent selectivity in the presence of 12 commonly existing interference gases for NO_2 detection. Given that the organic functional groups on OMCs can be flexibly designed for different gas detection purposes, our work should provide great inspiration in designing and producing the next generation of highly selective and sensitive sensing materials for RT operation.

This work was supported by the NSF of China (21822109, 21975254, 21805276, 21905280), the Key Research Program of Frontier Science, CAS (QYZDB-SSWSLH023), the Strategic Priority Research Program of CAS (XDB20000000), the International Partnership Program of CAS (121835KYSB201800), and the Youth Innovation Promotion Association CAS.

Conflicts of interest

There are no conflicts to declare.

Notes and references

1 E. Comini, C. Baratto, G. Faglia, M. Ferroni, A. Vomiero and G. Sberveglieri, *Prog. Mater. Sci.*, 2009, **54**, 1.
2 S. Chen, Y. Tang, K. Zhan, D. Sun and X. Hou, *Nano Today*, 2018, **20**, 84.
3 Y. Liu, R. Bao, J. Tao, J. Li, M. Dong and C. Pan, *Sci. Bull.*, 2020, **60**, 70.
4 V. Dua, S. P. Surwade, S. Ammu, S. R. Agnihotra, S. Jain, K. E. Roberts, S. Park, R. S. Ruoff and S. K. Manohar, *Angew. Chem., Int. Ed.*, 2010, **49**, 2154.
5 E. Singh, M. Meyyappan and H. S. Nalwa, *ACS Appl. Mater. Interfaces*, 2017, **9**, 34544.
6 J. Feng, L. Peng, C. Wu, X. Sun, S. Hu, C. Lin, J. Dai, J. Yang and Y. Xie, *Adv. Mater.*, 2012, **24**, 1969.
7 F. K. Perkins, A. L. Friedman, E. Cobas, P. M. Campbell, G. G. Jernigan and B. T. Jonker, *Nano Lett.*, 2013, **13**, 668.
8 W. Yuan, A. Liu, L. Huang, C. Li and G. Shi, *Adv. Mater.*, 2013, **25**, 766.
9 S. Y. Cho, Y. Lee, H. J. Koh, H. Jung, J. S. Kim, H. W. Yoo, J. Kim and H. T. Jung, *Adv. Mater.*, 2016, **28**, 7020.
10 S. Y. Cho, H. J. Koh, H. W. Yoo and H. T. Jung, *Chem. Mater.*, 2017, **29**, 7197.
11 M. G. Campbell, D. Sheberla, S. F. Liu, T. M. Swager and M. Dincă, *Angew. Chem., Int. Ed.*, 2015, **54**, 4349.
12 M. G. Campbell, S. F. Liu, T. M. Swager and M. Dincă, *J. Am. Chem. Soc.*, 2015, **137**, 13780.
13 M. K. Smith and K. A. Mirica, *J. Am. Chem. Soc.*, 2017, **139**, 16759.
14 Y. Ding, Y. P. Chen, X. Zhang, L. Chen, Z. Dong, H. L. Jiang, H. Xu and H. C. Zhou, *J. Am. Chem. Soc.*, 2017, **139**, 9136.
15 R. Dong, Z. Zhang, D. C. Tranca, S. Zhou, M. Wang, P. Adler, Z. Liao, F. Liu, Y. Sun, W. Shi, Z. Zhang, E. Zschech, S. C. B. Mannsfeld, C. Felser and X. Feng, *Nat. Commun.*, 2018, **9**, 2637.
16 M. Zhao, Y. Huang, Y. Peng, Z. Huang, Q. Ma and H. Zhang, *Chem. Soc. Rev.*, 2018, **47**, 6267.
17 M. S. Yao, J. J. Zheng, A. Q. Wu, G. Xu, S. S. Nagarkar, G. Zhang, M. Tsujimoto, S. Sakaki, S. Horike, K. Otake and S. Kitagawa, *Angew. Chem., Int. Ed.*, 2020, **59**, 172.
18 W. T. Koo, J. S. Jang and I. D. Kim, *Chem*, 2019, **5**, 1938.
19 M. S. Yao, X. J. Lv, Z. H. Fu, W. H. Li, W. H. Deng, G. D. Wu and G. Xu, *Angew. Chem., Int. Ed.*, 2017, **56**, 16510.
20 M. S. Yao, J. W. Xiu, Q. Q. Huang, W. H. Li, W. W. Wu, A. Q. Wu, L. A. Cao, W. H. Deng, G. E. Wang and G. Xu, *Angew. Chem., Int. Ed.*, 2019, **58**, 14915.
21 Z. Meng, R. M. Stolz and K. A. Mirica, *J. Am. Chem. Soc.*, 2019, **141**, 11929.
22 S. J. Choi and I. D. Kim, *Electron. Mater. Lett.*, 2018, **14**, 221.
23 Z. Meng, R. M. Stolz, L. Mendecki and K. A. Mirica, *Chem. Rev.*, 2019, **119**, 478.
24 F. Yavari, E. Castillo, H. Gullapalli, P. M. Ajayan and N. Koratkar, *Appl. Phys. Lett.*, 2012, **100**, 203120.
25 B. Cho, A. R. Kim, Y. Park, J. Yoon, Y. J. Lee, S. Lee, T. J. Yoo, C. G. Kang, B. H. Lee, H. C. Ko, D. H. Kim and M. G. Hahm, *ACS Appl. Mater. Interfaces*, 2015, **7**, 2952.
26 K. Lee, R. Gatensby, N. McEvoy, T. Hallam and G. S. Duesberg, *Adv. Mater.*, 2013, **25**, 6699.
27 J. S. Kim, H. W. Yoo, H. O. Choi and H. T. Jung, *Nano Lett.*, 2014, **14**, 5941.
28 Y. H. Kim, J. S. Park, Y. R. Choi, S. Y. Park, S. Y. Lee, W. Sohn, Y. S. Shim, J. H. Lee, C. R. Park, Y. S. Choi, B. H. Hong, J. H. Lee, W. H. Lee, D. Lee and H. W. Jang, *J. Mater. Chem. A*, 2017, **5**, 19116.
29 Y. Z. Li, J. Shu, Q. Q. Huang, K. Chiranjeevulu, P. N. Kumar, G. E. Wang, W. H. Deng, D. Tang and G. Xu, *Chem. Commun.*, 2019, **55**, 10444.
30 Y. Z. Li, X. M. Jiang, Z. H. Fu, Q. Q. Huang, G. E. Wang, W. H. Deng, C. Wang, Z. Z. Li, W. J. Yin, B. L. Chen and G. Xu, *Nat. Commun.*, 2020, **11**, 261.
31 L. G. Dance, K. J. Fisher, R. M. Herath Banda, M. L. Scudder, R. M. Herath Banda and M. L. Scudder, *Inorg. Chem.*, 1991, **30**, 183.
32 H. Yu, P. Xiao, J. Tian, F. Wang and J. Yu, *ACS Appl. Mater. Interfaces*, 2016, **8**, 29470.
33 K. H. Low, V. A. Roy, S. S. Chui, S. L. Chan and C. M. Che, *Chem. Commun.*, 2010, **46**, 7328.
34 M. S. Yao, W. X. Tang, G. E. Wang, B. Nath and G. Xu, *Adv. Mater.*, 2016, **28**, 5229.
35 M. W. G. Hoffmann, J. D. Prades, L. Mayrhofer, F. Hernandez-Ramirez, T. T. Järvi, M. Moseler, A. Waag and H. Shen, *Adv. Funct. Mater.*, 2014, **24**, 595.
36 J. S. Kim, J. W. Yoon, Y. J. Hong, Y. C. Kang, F. Abdel-Hady, A. A. Wazzan and J. H. Lee, *Sens. Actuators, B*, 2016, **229**, 561.
37 G. W. Peterson, J. J. Mahle, J. B. DeCoste, W. O. Gordon and J. A. Rossin, *Angew. Chem., Int. Ed.*, 2016, **55**, 6235.
38 E. Flores, J. Viallon, P. Moussay, F. Idrees and R. I. Wielgosz, *Anal. Chem.*, 2012, **84**, 10283.
39 C. Yu, H. Z. Lin, J. Zhou, X. F. Cheng, J. H. He, H. Li, Q. F. Xu, N. J. Li, D. Y. Chen and J. M. Lu, *J. Mater. Chem. A*, 2020, **8**, 1052.
40 B. Tyagi, C. D. Chudasama and R. V. Jasra, *Spectrochim. Acta, Part A*, 2006, **64**, 273.
41 G. C. Guo, Y. G. Yao, K. C. Wu, L. Wu and J. S. Huang, *Prog. Chem.*, 2001, **13**, 151.
42 S. P. Guo, Y. Chi and G. C. Guo, *Coord. Chem. Rev.*, 2017, **335**, 44.
43 G. W. Peterson, M. McEntee, C. R. Harris, A. D. Klevitch, A. W. Fountain, J. R. Soliz, A. Balboa and A. J. Hauser, *Dalton Trans.*, 2016, **45**, 17113.